

UV light influences covid-19 activity through big data : trade offs between northern subtropical, tropical, and southern subtropical countries

Novanto Yudistira,^{1*} Sutiman B. Sumitro,² Alberth Nahas,³ Nelly Florida
Riama⁴

¹*Intelligent System Lab, Faculty of Computer Science, University of Brawijaya,
Indonesia*

²*Faculty of Mathematics and Natural Science, University of Brawijaya, Indonesia*

³*Global Atmosphere Watch Station Bukit Kototabang the Indonesian Agency for
Meteorology, Climatology, and Geophysics, Indonesia*

⁴*Center for Research and Development, the Indonesian Agency for Meteorology,
Climatology, and Geophysics, Indonesia*

**To whom correspondence should be addressed; E-mail: yudistira@ub.ac.id*

Abstract

UV (ultraviolet) light is an important factor should be considered to predict coronavirus epidemic growth pace. UV is different from weather temperature since UV is electromagnetic wavelength from 10 nm to 400 nm in size, shorter than of visible lights. For some people, UV light can lead to cancer from unprotected sun exposure, however, for tropical people, which have been used to live in such condition, have resisted from negative effect high UV index. Moreover, UV has the capability to inactivate virus. This conclusion has been discussed deeply with biological experts. Although UV light has the ability to inactivate viruses, it may be meaningless in areas with high air pollution where UV light turns into heat. The data visualization code is available here <https://github.com/cbasemaster/uvcorona>

Keywords: Science, Publication, Complicated

1. Introduction

2 Coronavirus disease 2019 (Covid-19) was first detected in Hubei province
3 of China by Wuhan Municipal Health Commission and early information
4 about outbreak has been sent to World Health Organization (WHO) [1][2].

Preprint submitted to Journal Name

May 22, 2020

5 Disease capability to spread among communities are increased rapidly as the
6 number of people that exposed to covid-19 is increasing. This regards ev-
7 idence of human-to-human transmission indicating that covid-19 is highly
8 contagious. Moreover, covid-19 can also actively live airborne and in sur-
9 face [3]. These kind of transmissions can form pandemics. Pandemics can
10 cause severe mobility and mortality over wide geographic area [4]. However,
11 the efforts to halt covid-19 spread reduce carbon emission[5] of which ad-
12 vantageous for environment. To withstand spread of covid-19, one natural
13 instrument that rarely discussed is ultraviolet (UV). There are many UV
14 papers prove that it has capability to inactivate virus [6][7]. An example
15 about virus inactivation by UV is viral inactivation using UV-C irradiation
16 [8]. Even though UV has the ability to inactivate the virus but if the
17 pollution is high it will be meaningless [9]. Note that smoke particulate
18 is able to weaken the UV light ability to exist in the air [10]. Moreover,
19 The vaccine development is not effective and taking a long time to be found
20 [11]. Therefore, urgent, massive and natural immune are somewhat more
21 desirable. Previously, some technologies have been developed by making
22 use of UV light [12][13][14]. By aforementioned evidences, we investigate
23 how UV is related to geographical locations and the spread of covid-19 in
24 the world starting from Indonesia. Our assumption is that there is advan-
25 tage of country like Indonesia where UV index is very high to withstand
26 the spread of covid-19. As information, data sets of world confirmed covid-
27 19, UV index time series, pollution time series, and UV index of Indone-
28 sia are gathered from www.github.com/datasets/covid-19/tree/master/data,
29 www.temis.nl/uvradiation/UVarchive [15], www.aqicn.org, and BMKG (Me-
30 teorology, Climatology, and Geophysical Agency) www.bmkg.org, respec-
31 tively during 2020-01-22 to 2020-03-28.

32 *1.1. How UV index is determined*

33 The UV index is derived from the measured solar radiation in the UV
34 spectra that arrives on the surface. It is calculated by considering the pro-
35 portional contribution of both UV-A and UV-B, two of the three wavelength-
36 based types of UV radiation. UV-A is characterized as the UV radiation of
37 which the wavelength ranges from 280-315 nm, while the wavelength of UV-B
38 is between 315 nm and 400 nm.

39 The determination of UV index stems from the importance of its health
40 impacts to humans. Therefore, this index was developed to assess how the
41 exposure of excessive UV radiation may be detrimental particularly to the

42 exposed body. Both UV-A and UV-B have this damaging capability if the
43 exposure is not being taken cautiously. However, there are some differences
44 when it comes to the health effects by each type of UV radiation.

45 When determining the UV index, the contribution of UV-A and UV-
46 B is translated by implementing the weighting factors for individual UV
47 types. These factors were introduced by [16] to account for the amount of
48 received UV radiation on surface and the attributed energy of each UV type.
49 This level of energy is indicative of how damaging the exposure might be
50 experienced by a person. In general, UV radiation at longer wavelengths is
51 received more abundantly than that at shorter wavelengths. In other words,
52 more UV-A arrives on the surface than UV-B. However, the energy carried by
53 UV-A is less than that by UV-B because of the inverse relationship between
54 the energy amount and the radiation wavelength.

55 The weighting factors for determining the UV index accommodate both
56 the amount of received UV radiation and carried energy. A study by [16] has
57 provided a list of weighting factors for each nm wavelength of UV-A and UV-
58 B, with decreasing values assigned from lower to higher wavelengths (*i.e.*, the
59 weighting factors for UV-B are higher than those of UV-A). These factors
60 are utilized to account for how much UV energy received on the surface that
61 might affect the human health.

62 In the ideal situation, the application of the weighting factors to UV-A
63 and UV-B radiation is performed for each nm of wavelengths. However, data
64 from UV radiation is usually reported as a total of integrated UV radiation
65 from a range of wavelengths. As a result, applying the weighting factors
66 cannot be done to specifically determine the contribution of UV radiation
67 from every wavelength. With this compromised situation, an alternative
68 approach has been undertaken to select a weighting factor for a particular
69 wavelength that represents each UV-A and UV-B wavelength range. Since
70 the chosen wavelength can be arbitrary, some reasonable assumptions were
71 provided to serve as justification of calculation. For UV-A, the weighting
72 factor used was selected for the wavelength of 325 nm (UV-A weighting
73 factor = 0.0029). Although UV radiation from this wavelength penetrates to
74 the surface less than that from longer wavelengths, it has a higher weighting
75 factor that might be considered as a surrogate for other wavelengths.

76 Meanwhile for UV-B, the selected weighting factor was for 305 nm (UV-B
77 weighting factor = 0.22). This wavelength is located near the end of the UV-
78 B spectrum, indicating a lower energy amount than the other shorter UV-B
79 wavelengths. However, much of the shorter wavelengths are already absorbed

80 by gases in the atmosphere before arriving at the surface. Therefore, it can
81 be assumed that the prevalent UV-B radiation received on the surface is
82 from the longer wavelengths. In addition, the weighting factor for 305 nm is
83 located in the middle area of the UV-B longer wavelength spectrum, which
84 is appropriate to represent this range in calculation.

85 After applying the weighting factors to both UV-A and UV-B, the com-
86 bined energy is then used to determine the UV index. The UV index is
87 mathematically expressed by the following Eq. (1):

$$UVindex = \frac{UV_A + UV_B}{0.025} \quad (1)$$

88
89 where both UV-A and UV-B are expressed in $W\ m^{-2}$. The denominator
90 $0.025\ W\ m^{-2}$ is the standardized increment value that corresponds to how
91 much UV radiation can potentially be damaging to life tissues. In other
92 words, an increase of one UV index is equivalent to $25\ mW\ m^{-2}$ of exposed
93 UV radiation.

94 *1.2. Information of UV index in Indonesia*

95 UV radiation is one of the solar radiation components pertinent in de-
96 termining the atmospheric dynamics. Therefore, this parameter has been an
97 integral parameter to be measured on the surface. However, there is still a
98 limited number of ground-based measurements of UV radiation in Indone-
99 sia. Right now, the Indonesian Agency for Meteorology, Climatology, and
100 Geophysics (BMKG) operates a UV radiometer to measure UV radiation in
101 three climatological stations. These three locations, shown in SM2a, report
102 the incidence UV radiation received on the surface per hour. These values
103 are useful to determine the daytime UV radiation profile in each location.

104 The limitation of ground-based data for UV radiation poses some chal-
105 lenges in determining UV index for a country like Indonesia. However, this
106 limitation can be addressed by utilizing model-based UV radiation informa-
107 tion. Such information, for example, can be obtained from the European
108 Centre for Medium-Range Weather Forecast (ECMWF) UV radiation prod-
109 ucts. ECMWF releases two near real-time global UV radiation products,
110 which are UV biologically effective dose (uvbed) and UV biologically effec-
111 tive dose for clear sky (uvbed). The horizontal resolution of these products
112 is 0.4by 0.4, which is roughly equivalent to 40 km by 40 km. Both products
113 are adjusted UV radiation received on the surface that take into account

114 atmospheric and surface conditions, such as surface albedo, clouds, aerosol
115 loads, and surface ozone. Their values are analogue to the total weighted UV
116 radiation described earlier. As such, these products can also be converted
117 into a UV index by dividing the values by 0.025 W m^{-2} .

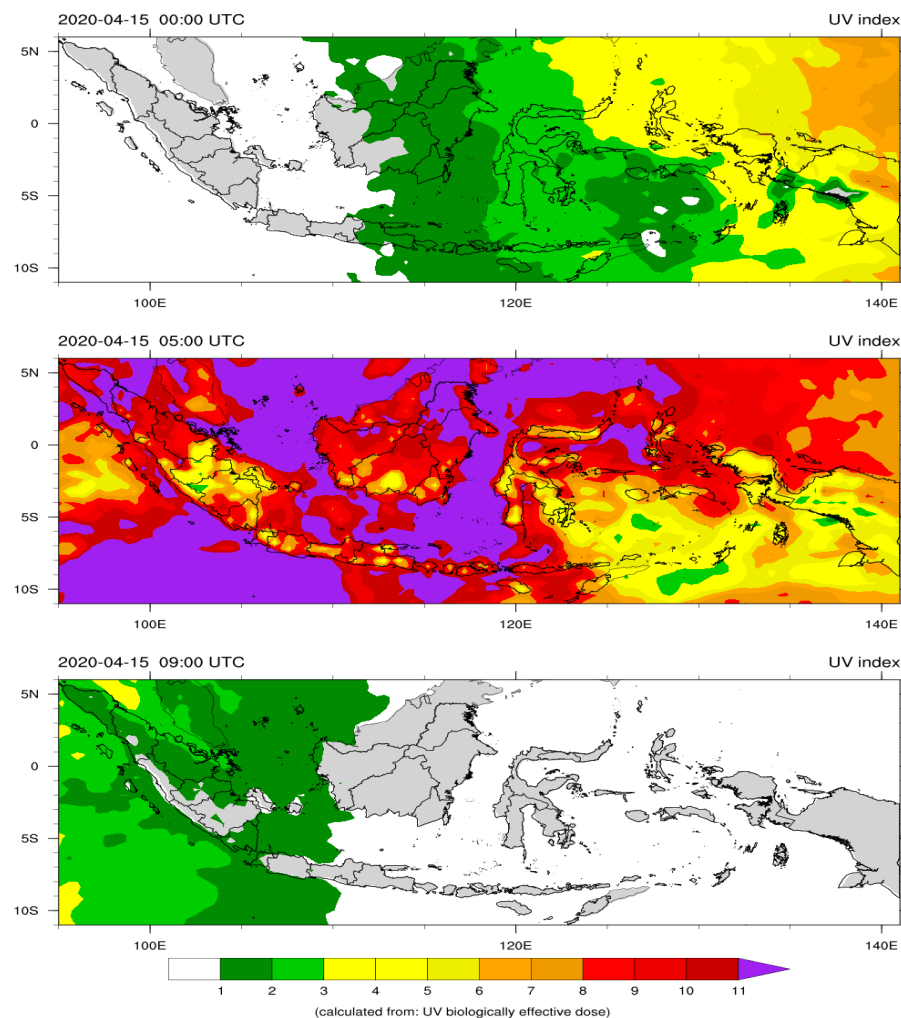


Figure 1: The spatial variation of UV index calculated from the ECMWF's uvbed product for April 15, 2020.

118 The spatial variation of UV index calculated from the ECMWF's uvbed
119 product for April 15, 2020, is depicted in fig. 1. In this figure, three selected

120 hours (*i.e.*, 0 UTC, 5 UTC, and 9 UTC, where Jakarta Time is seven hours
121 ahead of UTC) are shown to observe the changing of UV index from morning
122 to afternoon. At 0 UTC or 7 AM Jakarta Time, the central and eastern
123 parts of Indonesia have observed UV index 1 to 3, while most of the western
124 part was yet to be affected by UV radiation. As the day progressed and
125 the sun was overhead, most of the Indonesian region was under UV index
126 7 and above by 5 UTC or noon Jakarta time. In the afternoon, as the
127 sun was observed at a slanted angle, the UV index was either decreased or
128 zero. These changes of UV index are typical for daily observation. There
129 are some seasonal variations in terms of magnitude that is related to the
130 geometry between the sun and the earth. In addition, surface conditions and
131 atmospheric dynamics contribute to determining the UV index.

132 *1.3. UV index model vs observation: a comparative analysis*

133 In this study, the two ECMWF UV products were used as a comparison
134 to the ground-based data collected from the three locations for the period
135 of January to March 2020. After calculating the UV index from both ob-
136 servation and model data sets, daytime hourly UV indices were analyzed
137 to indicate whether there is an agreement between the two data sets. The
138 comparison from the three locations can be seen in fig. 2b - d.

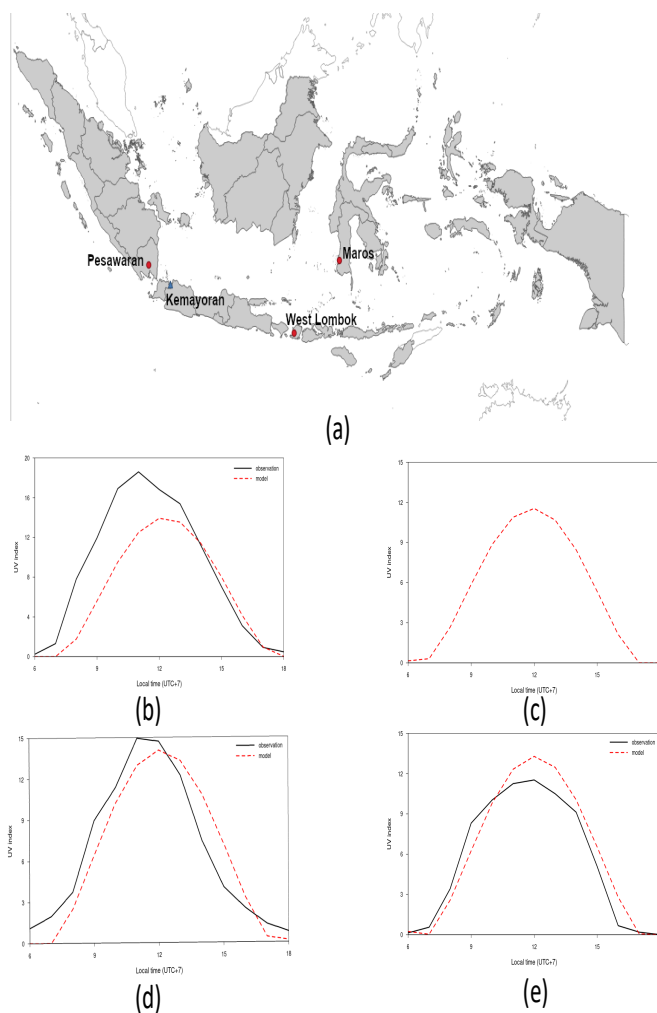


Figure 2: (a).ground-based data collected from the three locations (Pesawaran, Maros, and West Lombok) for the period of January to March 2020 (b). mean hourly UV indices in West Lombok Province. (c). T mean hourly UV indices in Kemayoran, Jakarta Province. (d). mean hourly UV indices in Maros, South Sulawesi. (e). mean hourly UV indices in Pesawaran, Lampung Province.

139 Fig. 2e and 2d show mean hourly UV indices in Pesawaran, Lampung
140 Province, and in Maros, South Sulawesi Province, respectively. It can be
141 observed that, in general, the model is able to capture the hourly pattern of
142 UV indices calculated from measured UV radiation. There are some slight
143 differences on the estimated UV indices, which might be attributed to the

144 coarse horizontal resolution of the model that did not include the dynamics
145 of atmospheric conditions on a finer scale. Nevertheless, these results can be
146 considered as a good agreement between the observation and the model.

147 A different result, however, is shown in 2b, where West Lombok in West
148 Nusa Tenggara Province observed the UV index difference between the model
149 and the observation. During its peak, the model underestimates the observa-
150 tion by more than five units. There are two factors that might be contributed
151 to this difference. Firstly, the model was not able to capture the local char-
152 acteristics of UV radiation received on the surface in this location. These
153 local characteristics can be associated with the topographical features and
154 the predominant weather conditions in this location. Secondly, the selection
155 of weighting factors to adjust UV-A and UV-B radiation is not suitable for
156 this location. It is possible that the UV radiation received on the surface
157 is at different wavelengths from one place to another. The absorption of
158 UV radiation is governed by atmospheric compositions and weather condi-
159 tions. Therefore, the amount of energy brought by UV radiation is subject
160 to at what wavelength the radiation is able to reach the surface. This re-
161 sult highlights the importance of future studies that involve more precise
162 measurements on UV radiation from different wavelengths. These studies
163 are required to determine the prevalent wavelength of UV radiation that is
164 measured on the ground.

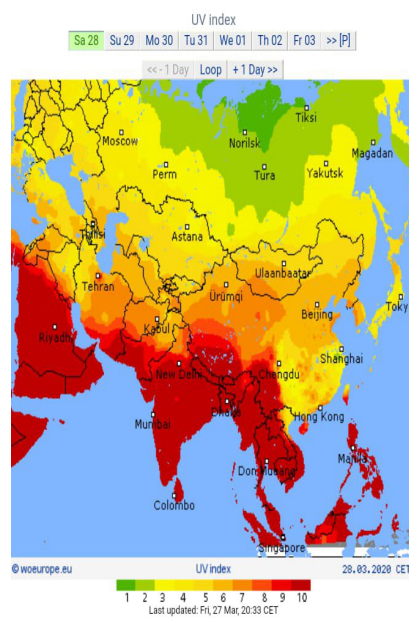
165 Notwithstanding the disagreement between the model and the observa-
166 tion shown in 2b, these results suggest an encouraging finding that the model
167 may be suitable for estimating the UV index in locations where there is no
168 ground-based data. This is of particular importance because of the limitation
169 of measurement availability in Indonesia. However, this method and its in-
170 terpretation have to be approached with cautions because of there is still
171 a need to get more information on the prevalent UV wavelength discussed
172 earlier.

173 Next, we look into the pattern of daily confirmed cases and UV index in
174 several countries. As a remainder, UV index can be measured as below :

- 175 • 0 to 2: Low Risk of harm from unprotected sun exposure.
- 176 • 3 to 5: Moderate Risk of harm from unprotected sun exposure.
- 177 • 3 to 5: Moderate Risk of harm from unprotected sun exposure
- 178 • 6 to 7: High Risk of harm from unprotected sun exposure

- 179 • 8 to 10: Very High Risk of harm from unprotected sun exposure
180 • 11+: Extreme Risk of harm from unprotected sun exposure

181 It possibly harms to people that are not used to live in such an extreme
182 UV index [17], however, it can reduce virus activity. The people who live in
183 high UV index areas such as Africa and other tropical countries have already
184 long-adapted in such situation. They may take advantage that pandemics
185 are not as excessive as subtropical countries.



(a)



(b)

Figure 3: (a). Visualization of uv index distribution over continents (woeurope.eu). (b). Visualization of confirmed covid-19 cases over continents (John Hopkins University Medicine on April 4, 2020).

186 1.4. *Difference UV between tropical location and covid-19 pandemic growth*

187 Fig. 3a shows uv index over the Asia and Europe on March 28 2020 that
188 seems to be correlated to covid-19 pandemic rate over countries on April 4
189 2020 (3b). Most of high rate of covid-exposed countries are located in sub-
190 tropical area, conversely, low rate of covid-exposed countries are spreading

191 throughout tropical areas. Concurrently, tropical countries have high index
192 of UV index (> 7) over time whilst subtropical countries are interchanging
193 between low (< 4) and high index (> 7) of UV index depending on the sea-
194 son. The confirmed cases map in Fig.1a seems to be correlated to UV index
195 map where the majority of confirmed people live in the northern subtropical
196 countries (fig. 3b). The southern subtropical countries are still in low rate
197 of pandemic growth, however, the earth is revolutionize and between May to
198 August they are gradually entering cold season with low level pf UV index.
199 They have advantages of early anticipation of covid-19 growth in situation
200 where UV index is still high.

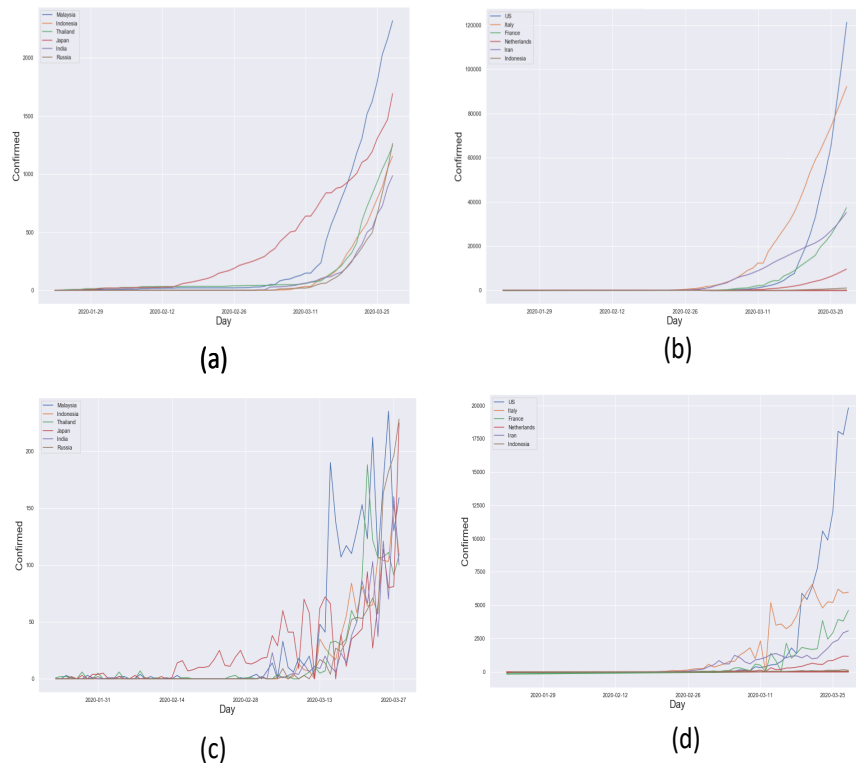


Figure 4: (a). The pandemic growth of countries which have low level of growth rate. It is shown that confirmed accumulation in range of 0–2000+ people. (b). The pandemic growth of countries which have low level of growth rate. It is shown that confirmed accumulation in range of 0–120000+ people. (c). Daily confirmed case in low growth rate countries. (d). Confirmed case per day in some countries

201 *1.5. How coronavirus spreads differently in each country*

202 Coronavirus which causes the illness known as covid-19 was first reported
203 in China in December 2019. By March 28 2020, this disease has been spread-
204 ing to at least 178 countries and territories. In some countries, the accumu-
205 lation of confirmed cases varies from 0 to more than 120000 people over time
206 (fig. 4a and 4b). This data shows that this virus has the ability to spread
207 easily and quickly. Indonesia as one of the countries affected by coronavirus

208 shows the number of cases climbing to 1000 people. The number seems to be
 209 high but it is still lower when compared to other countries such as America,
 210 Italy, France, Netherlands, and Iran.

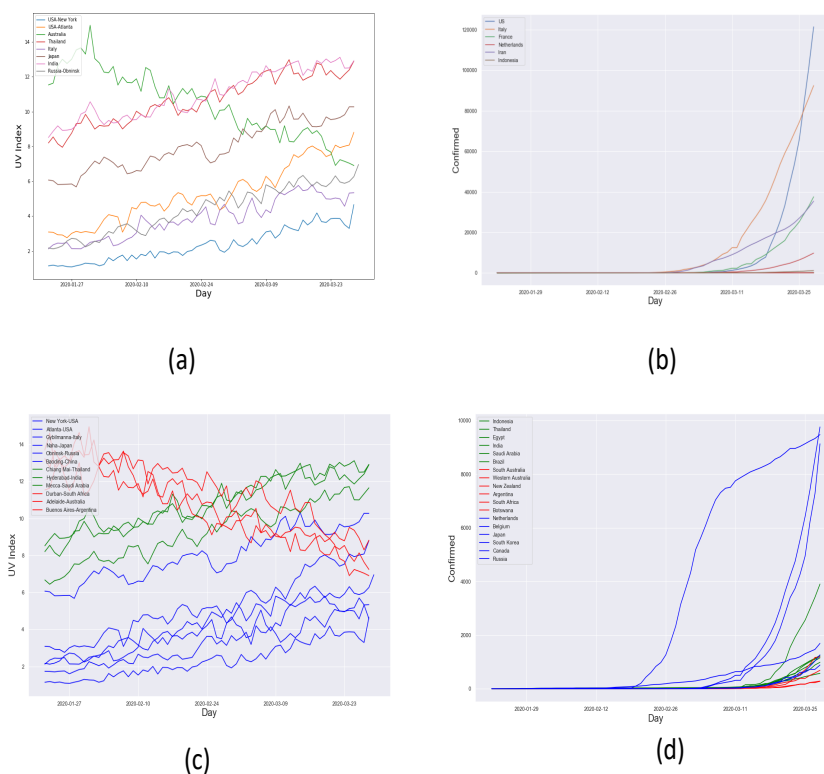


Figure 5: (a).UV Index over time in many countries. (b). The pandemic growth of countries. (c). The UV index alteration over time in northern sub tropical countries (blue), tropical countries (green), and southern sub tropical countries (red). (d). The covid-19 pandemic growth in northern sub tropical countries (blue), tropical countries (green), and southern sub tropical countries (red). Note that US, UK, Italy, or Spain is not included due to very high growth rate.

211 Fig. 4a and 4b show the spread of coronavirus in some countries that less
 212 than 5000 confirmed cases and more than 5000 confirmed cases, respectively.
 213 The accumulation of confirmed case grows exponentially with different rate

214 in each country. Indonesia grows in very little rate compared to US, Italy,
215 France, Netherlands, and Iran. We can easily cluster those countries by its
216 location using pandemic growth information. For example, referring to Fig.
217 3a and 3b, Malaysia, Indonesia, Thailand, and India can be grouped into
218 one cluster while US, Italy, France, Netherlands, Iran, Japan, and Russia in
219 another cluster by its tropical and subtropical continent, respectively. Japan,
220 however, has higher UV index compared to US, Italy, and Russia and its UV
221 index grows over time as spring season is coming (fig. 5a). Russia that has
222 low population density seems to have anomaly here and of course another
223 parameter such as humidity, air pollution or even economic relation with
224 epicentre country can be taken into account in future studies (update: by
225 May 22 2020, the total of conformed cases in Russia is positioned at second
226 after US).

227 *1.6. Daily cases vs UV index*

228 Before, let us show the covid-19 epidemic growth in several countries and
229 how exponential its slope between January 22 2020 to March 28 2020. The
230 number of confirmed cases of people infected with the corona virus tends
231 to increase every day (fig. 4c and 4d). This trend shows how quickly this
232 virus transmits among humans. Inside human body, this virus takes time
233 to show symptoms of illness. it makes coronavirus easily spreading among
234 people before the carrier notice about it. Highest confirmed case reported in
235 US reaches around 20000 people in a day on March 28 2020 (Fig. 4d).

236 Based on the fig. 5a, during the same days with pandemic growth in
237 fig. 5b, northern subtropical countries have UV index grows over time as the
238 cold season ended and spring season is coming. Australia as a representation
239 of subtropical countries has its UV index decreasing over time as summer
240 season ended and fall season is coming. In Atlanta, area which is located in
241 central area of US, has higher UV index than of in New York, even though
242 they both grow concurrently over time. Interestingly, New York area has
243 lowest UV index compared to others of which has UV index of 1 to 4 over
244 time. In tropical countries, such as Thailand and India, UV index tends to
245 be stable over time during January 22 2020 to March 28 2020.

246 *1.7. Tropical vs Subtropical : interesting characteristics*

247 Fig.5d shows pandemic growth in tropical (green), northern subtropical
248 (blue), and southern subtropical (red). It is quite interesting that the blue
249 countries grow exponentially over time since the initially confirmed people

250 are recorded, with sharper, and faster than the green and red countries. The
251 green countries grow sharper and faster than red countries, even though the
252 growth of some countries has cross points with each other. The overtaking
253 points indicate that there exist growth pace that is becoming slower than the
254 other, and vice versa. This happens between two adjacent groups either blue
255 with green or green with red. This phenomenon possibly can be explained
256 in Fig.5c.

257 Fig.5c shows the change of UV index over time in northern subtropical
258 countries (blue), tropical countries (green), and southern tropical countries
259 (red). We can easily understand that the blue and green countries are mono-
260 tonically increasing over time while the red countries are monotonically de-
261 creasing. This phenomenon regards the changing season between cold to
262 summer in northern countries and, conversely from summer to cold season
263 in southern tropical countries. The green countries rarely have UV Index
264 below 6. UV Index behavior of blue, green, and red countries are concurrent
265 with the accumulation of confirmed covid-19 over time in Fig.5d. Some blue
266 countries are starting to be sloppier as higher UV Index and with proper
267 social distancing.

268 Even though we still do not know the final growth curve, by the aforemen-
269 tioned evidence, they should prepare the worst case. The dynamic patterns
270 of the current situation show that some southern subtropical countries are
271 starting to grow exponentially as shown in Fig.5d. Especially, for airborne
272 covid-19 viruses that exist in the air, spreading vastly in the air. They can
273 perform early restrictions before exponential increase whilst also reduce pol-
274 lution to let UV lights reach the surface.

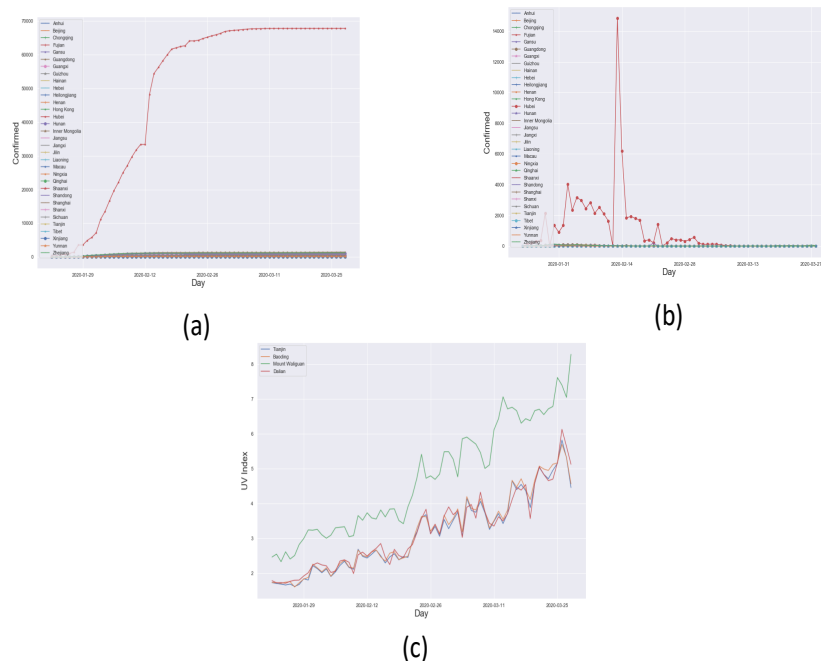


Figure 6: (a) Accumulation of confirmed case in China until the days of growth halt. (b). Daily confirmed case in China. (c). The UV index over time in China. The four stations are presented which are Tianjin and Dalian in northern China, Mount Waliguan in central China, and Baoding represents middle and southern China.

275 *1.8. China case : recovering with the help of UV light and lockdown?*

276 Fig.6a shows graphs of confirmed case accumulation over time in China.
 277 There is an interesting fact that Hubei province in which Wuhan city is lo-
 278 cated does not extremely spread covid-19 to other provinces. Fig. 6b shows
 279 graph of daily confirmed cases in China. There is also an interesting fact
 280 that Hubei province, in which Wuhan city is located, does not extremely
 281 spread covid-19 to other provinces. The daily confirmed cases show that
 282 other provinces do not show significant confirmed cases compared to Hubei

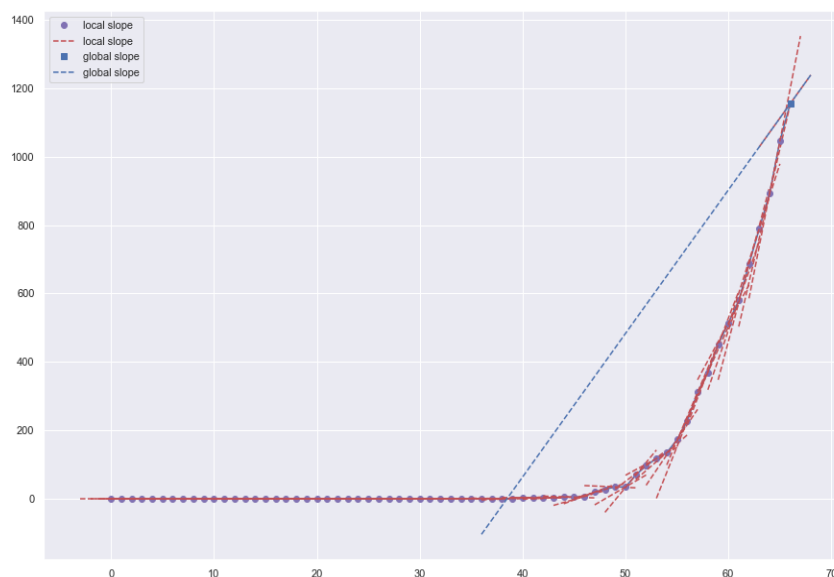


Figure 7: Example of local slopes and global slope

283 province. This is related to China government effort to carry out tight lock-
284 down in the epicentre (Hubei area) thorough screening, testing and contact
285 tracing programs, as well as bringing in early social distancing whilst also
286 light lockdown in another area [18]. The reason can be two-fold: the help of
287 lockdown with its social distancing and by the help of increasing UV index
288 as shown in Fig.6c. All four stations of Tianjin, Dalian, Mount Waliguan,
289 and Baoding show increased UV index over time during January 22 2020 to
290 March 28 2020.

291 *1.9. Growth Slope : see the change over time*

292 We use local and global slopes by means tangent line [7] as parameters to
293 see how related the UV index time series with the accumulation of confirmed
294 covid-19 growth as shown in fig. 7. tangent line is used as the steepness
295 metric of the graph. The tangent line is defined as follows:

$$y - y_1 = f'(x_1)(x - x_1) \quad (2)$$

296 Where f is growth function and x and x_1 are target and initial point,
297 respectively. The difference between local and global slope is that local slope
298 uses each local point in time frame relatives to initial point y_1 to estimate the
299 tangent line while the global slope is measured from the last point relatives
300 to initial point y_1 . The global slope gives more global growth performance.

301 *1.10. Correlation Test : to see the relationship between parameters*

302 Let me remind you that:

- 303 • 1.0 = positively correlated ; for instance, if A increases, B also increases,
304 and vice versa.
- 305 • 0.0 = no correlation ; for instance, if A increases, B does not change,
306 and vice versa.
- 307 • -1.0 = negatively correlated ; for instance, if A increases, B also de-
308 creases, and vice versa.

309 Let us introduce you to several parameters to be tested:

- 310 • UVIEF: cloud-free,erythemat (sunburn),UV index.
- 311 • UVDEF: cloud-free,erythemat (sunburn),UV dose,[kJ/m2].
- 312 • UVDDF: cloud-free,dna-damage,UV dose,[kJ/m2].
- 313 • UVDEC: cloud-modified,erythemat (sunburn),UV dose,[kJ/m2].
- 314 • ozone: local,solar,noon,ozone,column,[DU].

315 UV index is a measure for the effective UV irradiance (1 unit equals 25
316 mW/m2) reaching the Earth's surface in clear sky. UV dose is the effective
317 UV irradiance (given in kJ/m2) reaching the Earth's surface integrated over
318 the day and taking the attenuation of the UV radiation due to clouds into
319 account. Total column ozone is the total amount of ozone in a column ex-
320 tending vertically from the earth's surface to the top of the atmosphere. It is
321 measured using ground-based stations and satellites and is reported in Dob-
322 son units (DU). The ozone hole is defined in terms of reduced total column
323 ozone — less than 220 DU.

324 The correlation map between variables is defined as follows:

$$\forall corr_{mk} = \frac{\sum_{j=1}^N (a_{jm} - \bar{a}_m)(a_{jk} - \bar{a}_k)}{\sum_{j=1}^N (a_{jm} - \bar{a}_m)^2 \sum_{j=1}^N (a_{jk} - \bar{a}_k)^2} \quad (3)$$

325 Where for all available variables we calculate correlation between variables
 326 m and k .

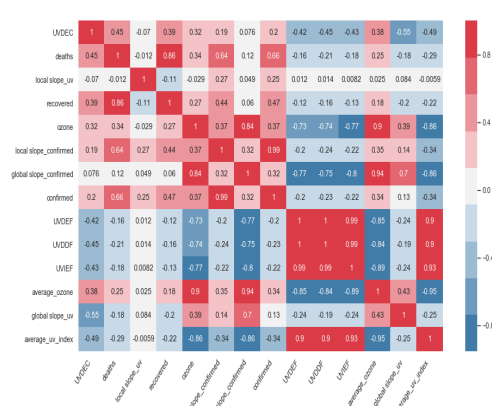
327 *1.11. Correlation test of the world data*

328 Countries to be included are Australia, Thailand, India, Japan, US, Italy.
 329 Global Atmosphere Watch (GAW) station to be used :

- 330 ● AcadiaNatForest,USA
- 331 ● Gibilmanna, Italy
- 332 ● Chiang Mai, Thailand
- 333 ● Hyderabad, India
- 334 ● Adelaide, Australia
- 335 ● Naha, Japan



(a)



(b)

Figure 8: (a) Correlation map between parameters of the world. (b). Correlation map between parameters of China.

336 Fig.8a shows correlation map between parameters of the world. Average
337 of UV index and average of ozone over time are correlated to global slope
338 of confirmed cases accumulation by -0.86 and 0.94, respectively. Meaning
339 that the higher UV Index is, the lower the growth rate of covid-19 pandemic
340 would be, and vice versa with a correlation of -0.86. Conversely, the higher
341 the ozone value is the higher growth rate of covid-19 pandemic would be,
342 and vice versa with a correlation of 0.94 as shown in fig. 8a. the global
343 slope of UV index alteration over time is correlated to the global slope of
344 confirmed cases accumulation by 0.7. This is understandable since the UV
345 index in northern subtropical countries tends to increase over time indicated
346 by high tangent value, however, the growth rate of covid-19 pandemic is still
347 increasing even though the pace is slowing down. Conversely, in southern
348 subtropical countries, the UV index tends to decrease over time making the
349 tangent value to be low even minus. We should wait for the next several
350 months to see whether southern subtropical countries will exponentially in-
351 crease the confirmed cases or not as data taken only until March 28, 2020.

352 *1.12. Correlation test of China data*

353 Provinces to be included are Tianjin, Hebei, Liaoning, Qinghai. GAW
354 station to be used :

- 355 • Tianjin
- 356 • Baoding
- 357 • Mount Waliguan
- 358 • Dalian

359 Fig. 8b shows correlation map between parameters of China. Average of
360 UV index and average of Ozone over time are correlated to global slope of
361 confirmed cases accumulation by -0.86 and 0.94, respectively. Meaning that
362 the higher UV Index is, the lower growth rate of covid-19 pandemic would
363 be, and vice versa with a correlation of -0.86. Conversely, the higher the
364 ozone value is the higher growth rate of covid-19 pandemic would be, and
365 vice versa with a correlation of 0.94 as shown in fig. 8b.

366 2. Discussion

367 Based on these findings, anticipation in form of gradual from loose to
368 tight in southern subtropical countries in accordance with UV index over
369 time might be taken into account to reduce the economic burden. Tropical
370 countries might take advantage of its high UV Index in the entire session
371 but has to keep anticipating. Special attention in the central economy area
372 where there is heavy air pollution should be considered because the high UV
373 index does not have enough potential to inactivate the virus. Meaning that
374 it should be anticipated that the exponential phase will be high.

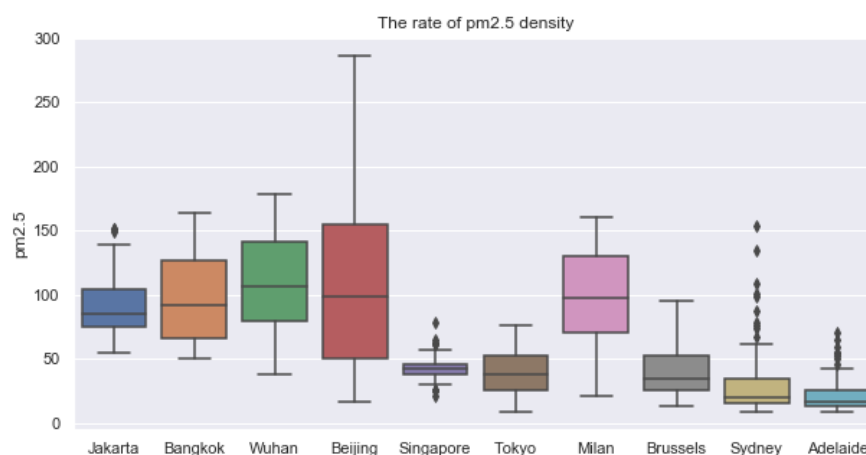


Figure 9: pm2.5 boxplots of epicenter cities during January to April.

375 As we can see in fig. 9, Jakarta, Bangkok, Wuhan, Beijing, and Milan have
376 higher pollution of PM2.5 than Singapore, Tokyo, Brussels. However, Sydney
377 and Adelaide have the lowest PM2.5 pollution. As remainder, PM2.5 is kind
378 of particulate matter produced from diesel exhausts, home cooking, smoke
379 from burning wood, etc. It is measured by microgram per cubic meter (Fig.
380 6). Low pollution corresponds to the best air quality index within the range of
381 January-April and concurrently with pm2.5 pollution rate, Australia has the
382 lowest rate of covid-19 exposure. Now, we try to correspond with data of UV
383 light time series within January to April. Sydney and Adelaide have a high
384 UV index while their pollution is at the lowest level compared to others of
385 which concurrent with low confirmed covid-19 cases in Australia. Moreover,

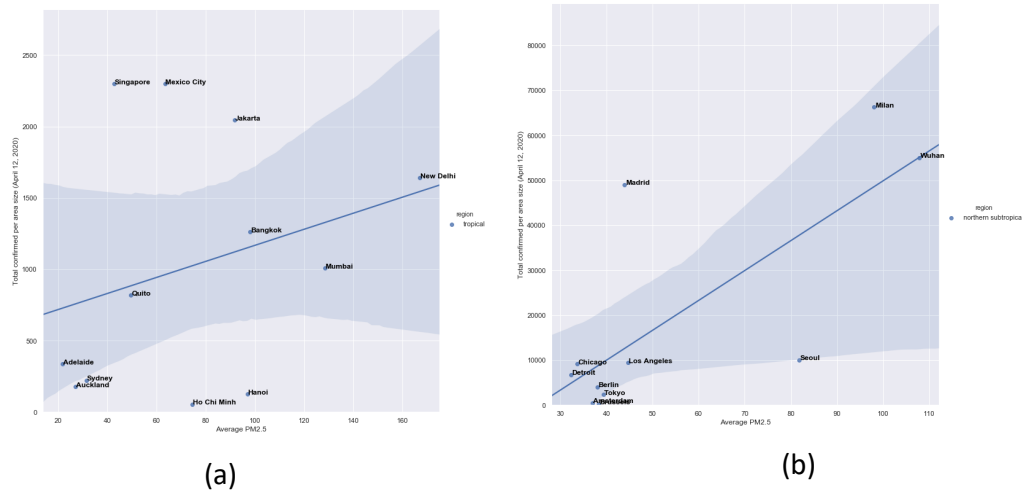


Figure 10: Regression analysis between confirmed cases and average of PM2.5 in (a) tropical and southern subtropical cities and (b) northern subtropical cities.

386 they also did an early anticipation by holding initial social distancing and
 387 another restrictions to facilitate medical experts to test, find, quarantine, and
 388 handle suspects as soon as possible. In northern subtropical cities, Brussels
 389 has low both UV index and pollution. In other hand, Milan (Italy) has high
 390 pollution whilst at the same time its condition is worsened with low UV
 391 index during that season, January until April. Tokyo has a moderately low
 392 UV index and pollution. In tropical city, Singapore has a moderately high
 393 UV index and pollution, however, remember that they have done tests to
 394 20815 / 1 million population dated on April 12 2020, a higher sampling rate
 395 than the others. In China, from January to February, Wuhan and Beijing
 396 have a high pollution level and gradually become lower starting from March
 397 to April, therefore, they have a longer standard deviation of average of pm2.5
 398 than the others. China is also recorded to have an upward UV index within
 399 the range of February-April based on UV light time series data in Fig. 6c.
 400 Another tropical cities, Jakarta and Bangkok have a high pollution rate with
 401 mean of pm2.5 rate is around 100, similar to Wuhan and Beijing, however,
 402 the UV index of Indonesia at that time is slightly lower than Thailand which
 403 regards the confirmed covid-19 case of Thailand is less than Indonesia even
 404 though located in the same tropical countries. Note that the epicenter of
 405 Indonesia and Thailand is Jakarta and Bangkok, respectively.

406 Now, we look into regression analysis between PM2.5 rate and total con-
407 firmed covid-19 cases on April 12 2020. We split cities to tropical and south-
408 ern subtropical cities (fig. 10a) and northern subtropical cities (fig. 10b).
409 This split follows assumption of UV index cluster during January to April.
410 The regression of tropical cities in fig. fig. 10a shows that they are positively
411 correlated. It is shown that we have an outlier of Jakarta, Singapore, Hanoi,
412 and Ho Chi Minh, however, Jakarta and Singapore are still higher than of
413 Adelaide, Sydney, and Auckland of which located in southern subtropical
414 countries. The problem of a developed country that confidently located in
415 the northern subtropical area is the high level of pm10 of which usually prod-
416 uct of factories. However, in cities, the problem of pm2.5 might still exist.
417 fig. 10b shows that Milan, Wuhan, Madrid, Los Angeles are in the same clus-
418 ter though it still has outliers of Seoul and Madrid. Chicago, Los Angeles,
419 Detroit, Berlin, Tokyo, and Amsterdam in another cluster. This result is in
420 line with number of confirmed covid-19 case where Wuhan, Milan, and Los
421 Angeles have higher accumulation number of confirmed covid-19.

422 Temperature and humidity possibly influence the covid-19 spread [19]. It
423 was found that greater survival of coronavirus occurs in lower temperature
424 and humidity. Based on its results, it is indicated that geographical locations
425 where higher temperature and humidity exist such as tropical countries have
426 advantages in withstanding the covid-19 spread. Humidity has greater role
427 in inactivating virus than temperature either on surface or in the air. It could
428 explain why some tropical countries has more confirmed covid-19 cases than
429 the others. These conclusions open up future research potential where UV,
430 pollution, and humidity can be strong features to predict and analyse the
431 spread of covid-19.

432 **3. Conclusion**

433 While UV index and ozone are correlated with global spread of corona
434 pandemic, we believe it is not just a standalone factor. There are some
435 other factors such as economic activity and population density influencing
436 the spread and growth of coronavirus cases. However, UV light and ozone
437 are strong enough to be taken into account to minimize the global covid-19
438 pandemic effect. In the cities where there is heavy air pollution, the high
439 UV index might be no meaning in terms of inactivating the virus. Next, we
440 would like to investigate on a smaller scale in one nation such as Indonesia
441 with humidity and pollution are included. Another thing is we are preparing

442 to predict when pandemics will end in each country using neural network
443 model.

444 **References**

- 445 [1] C. Wang, P. W. Horby, F. G. Hayden, G. F. Gao, A novel coronavirus
446 outbreak of global health concern, *The Lancet* 395 (2020) 470–473.
- 447 [2] D. Hui, I azhar e, madani ta, et al. the continuing 2019-ncov epidemic
448 threat of novel coronaviruses to global health-the latest 2019 novel coro-
449 navirus outbreak in wuhan, china, *Int J Infect Dis* 91 (2020) 264–266.
- 450 [3] N. Singh, M. Kaur, On the airborne aspect of covid-19 coronavirus,
451 arXiv preprint arXiv:2004.10082 (2020).
- 452 [4] N. Madhav, B. Oppenheim, M. Gallivan, P. Mulembakani, E. Rubin,
453 N. Wolfe, Pandemics: risks, impacts, and mitigation, in: *Disease
454 Control Priorities: Improving Health and Reducing Poverty*. 3rd edi-
455 tion, The International Bank for Reconstruction and Development/The
456 World Bank, 2017.
- 457 [5] E. Callaway, D. Cyranoski, S. Mallapaty, E. Stoye, J. Tollefson, The
458 coronavirus pandemic in five powerful charts., *Nature* 579 (2020) 482–
459 483.
- 460 [6] M. M. Jensen, Inactivation of airborne viruses by ultraviolet irradiation,
461 *Appl. Environ. Microbiol.* 12 (1964) 418–420.
- 462 [7] A. N. Strahler, Quantitative slope analysis, *Geological Society of Amer-
463 ica Bulletin* 67 (1956) 571–596.
- 464 [8] K. Bergmann, Uv-c irradiation: A new viral inactivation method
465 for biopharmaceuticals. *american pharmaceutical review*. consultado el
466 01/04/2020, 2014.
- 467 [9] P. Koronakis, G. Sfantos, A. Paliatsos, J. Kaldellis, J. Garofalakis, I. Ko-
468 ronaki, Interrelations of uv-global/global/diffuse solar irradiance compo-
469 nents and uv-global attenuation on air pollution episode days in athens,
470 greece, *Atmospheric Environment* 36 (2002) 3173–3181.

- 471 [10] W. F. Barnard, B. N. Wenny, Ultraviolet radiation and its interac-
472 tion with air pollution, in: *UV Radiation in Global Climate Change*,
473 Springer, 2010, pp. 291–330.
- 474 [11] R. Kuznia, The timetable for a coronavirus vaccine
475 is 18 months. experts say that’s risky, 2020. URL:
476 <https://edition.cnn.com/2020/03/31/us/coronavirus-vaccine-timetable-concerns-e>
- 477 [12] T. Koutchma, Advances in ultraviolet light technology for non-thermal
478 processing of liquid foods, *Food and Bioprocess Technology* 2 (2009)
479 138–155.
- 480 [13] K. N. Prodouz, J. C. Fratantoni, E. J. Boone, R. F. Bonner, Use of
481 laser-uv for inactivation of virus in blood products (1987).
- 482 [14] J. W. Tang, The effect of environmental parameters on the survival
483 of airborne infectious agents, *Journal of the Royal Society Interface* 6
484 (2009) S737–S746.
- 485 [15] J. Van Geffen, R. Van Der A, M. Van Weele, M. Allaart, H. Eskes,
486 Surface uv radiation monitoring based on gome and sciamachy, 2004.
- 487 [16] A. McKinlay, B. Diffey, W. Passchier, Human exposure to ultraviolet
488 radiation: risks and regulations, *Excerpta Medica*, Amsterdam, Nether-
489 lands (1987).
- 490 [17] K. Ezzedine, C. Guinot, E. Mauger, T. Pistone, M.-C. Receveur,
491 P. Galan, S. Hercberg, D. Malvy, Travellers to high uv-index coun-
492 tries: Sun-exposure behaviour in 7822 french adults, *Travel medicine*
493 and infectious disease 5 (2007) 176–182.
- 494 [18] Z. Wu, J. M. McGoogan, Characteristics of and important lessons from
495 the coronavirus disease 2019 (covid-19) outbreak in china: summary of
496 a report of 72 314 cases from the chinese center for disease control and
497 prevention, *Jama* 323 (2020) 1239–1242.
- 498 [19] L. M. Casanova, S. Jeon, W. A. Rutala, D. J. Weber, M. D. Sobsey,
499 Effects of air temperature and relative humidity on coronavirus survival
500 on surfaces, *Appl. Environ. Microbiol.* 76 (2010) 2712–2717.